

# The microwave dielectric properties of $\text{CaTiO}_3\text{--Li}_{0.5}\text{Nd}_{0.5}\text{TiO}_3$ ceramics prepared with $\text{Bi}_2\text{Ti}_2\text{O}_7$ additions

T. Lowe\*, F. Azough, R. Freer

Materials Science Centre, University of Manchester/UMIST, Grosvenor Street, Manchester, M1 7HS, UK

## Abstract

Ceramics of  $0.4\text{CaTiO}_3\text{--}0.6\text{Li}_{0.5}\text{Nd}_{0.5}\text{TiO}_3$  (0.4CT–0.6LNT) have been prepared by the mixed oxide route using additions of  $\text{Bi}_2\text{O}_3\text{--}2\text{TiO}_2$  (up to 30 wt.%). Powders were calcined  $1100^\circ\text{C}$ ; cylindrical specimens were fired at temperatures in the range  $1175\text{--}1275^\circ\text{C}$ . Sintered products were typically 90–95% dense. The microstructures were dominated by angular grains typically  $2\ \mu\text{m}$  in size. With increasing levels of  $\text{Bi}_2\text{O}_3\text{--}2\text{TiO}_2$  additions, needle and then lath shaped second phases developed. Microwave dielectric properties of 0.4CT–0.6LNT at 2.1 GHz were 126, 2600 GHz and 127 ppm/ $^\circ\text{C}$  for  $\epsilon_r$ , Qxf and  $\tau_f$ , respectively. The use of bismuth additions caused the relative permittivity to increase (to a maximum value of 150), the Qxf to steadily decrease (minimum value of 1000GHz) and  $\tau_f$  to decrease almost linearly towards zero.

© 2003 Elsevier Ltd. All rights reserved.

**Keywords:** Bismuth titanate;  $\text{CaTiO}_3$ ; Microwave dielectric; Perovskite

## 1. Introduction

The growth of the telecommunications industry over the past 15 years<sup>1</sup> has resulted in an increasing demand for the miniaturization of microwave components. Miniaturization can be achieved by increasing the relative permittivity ( $\epsilon_r$ ) since the size of microwave components is inversely proportional to the square root of the relative permittivity. Additional requirements are that the dielectric  $Q$  value is maximized (i.e. the dielectric losses minimized) and the dielectric properties be temperature stable such that the temperature coefficient of resonant frequency ( $\tau_f$ ) is maintained close to zero ( $\pm 5$  ppm/ $^\circ\text{C}$ ). In some cases, materials that have similar crystal structures but opposite temperature coefficients of resonant frequency, can be combined to produce a ceramic with the desired microwave properties and zero  $\tau_f$ .

During the last ten years, low loss ceramics in the system  $\text{CaTiO}_3\text{--Li}_x\text{Ln}_{1-x}\text{TiO}_3$  ( $\text{Ln} = \text{Sm}, \text{Nd}$ ) have attracted much interest<sup>2–5</sup> because of their high relative permittivity. The calcium end member  $\text{CaTiO}_3$  has  $\epsilon_r$  of 170 and Qxf value of 2000 GHz whilst  $\text{Li}_x\text{Sm}_{1-x}\text{TiO}_3$  has  $\epsilon_r = 80$  and Qxf = 2100. The  $\tau_f$  values of the two end members are non-zero, but of opposite polarity. Kim and Yoon<sup>2</sup> showed that good dielectric properties could

be obtained in the system  $\text{CaTiO}_3\text{--Li}_{0.5-3x}\text{Sm}_{0.5-x}\text{TiO}_3$  (CT–LST). However, Takashi et al.<sup>6</sup> demonstrated that the microwave dielectric properties in such systems vary with ionic size, so that replacing Sm with Nd (*increase in ionic radii*) should yield a ceramic with a higher relative permittivity. Therefore in the present study, the system  $\text{CaTiO}_3\text{--Li}_{0.5}\text{Nd}_{0.5}\text{TiO}_3$  has been investigated. The composition  $0.4\text{CaTiO}_3\text{--}0.6\text{Li}_{0.5}\text{Nd}_{0.5}\text{TiO}_3$  has been selected since it should yield materials with near zero  $\tau_f$  values. A number of authors<sup>7–9</sup> have indicated that  $\text{Bi}_2\text{O}_3$  has a beneficial influence upon the dielectric properties of the  $\text{BaO--Nd}_2\text{O}_3\text{--TiO}_2$  based ceramics. Bismuth tends to lead to an increase in relative permittivity and reduction in  $\tau_f$ , but also a reduction in the Qxf value. In this study the effect of  $\text{Bi}_2\text{Ti}_2\text{O}_7$  additions to  $0.4\text{CaTiO}_3\text{--}0.6\text{Li}_{0.5}\text{Nd}_{0.5}\text{TiO}_3$  has been examined.

## 2. Experimental

Ceramics of 0.4CT–0.6LNT were prepared by the mixed oxide route using  $\text{CaTiO}_3$  (99%—ALFA AESAR),  $\text{Li}_2\text{CO}_3$  (99%—Fluka),  $\text{Nd}_2\text{O}_3$  (99%—Honeywell Electronic Materials) and  $\text{TiO}_2$  (98.5%—Tioxide UK Ltd). For the additions of  $\text{Bi}_2\text{O}_3\text{--}2\text{TiO}_2$  (BT), powders of  $\text{Bi}_2\text{O}_3$  (99%—Fluka) and  $\text{TiO}_2$  (98.5%—Tioxide UK Ltd) were employed. The two sets of powders, 0.4CT–0.6LNT and BT, were mixed and processed

\* Corresponding author.

independently. Each was wet milled in propan-2-ol for 16 h, and then calcined at 1100 °C for 4 h. At the end of this stage, appropriate amounts of  $\text{Bi}_2\text{O}_3\text{-}2\text{TiO}_2$  (5–30 wt.%) were added to the stock 0.4CT–0.6LNT powder and individual batches were ball milled for a further 16 h. After drying, cylindrical samples were pressed at 50–100 MPa. In order to minimise lithium loss during firing, the specimens were surrounded in powder of the same composition and supported on a powder-covered alumina substrate. Sintering was performed in air at temperatures in the range of 1175 and 1275 °C for 3 h. The heating and cooling rates were 360 and –240 °C/h. Product densities were determined from weight and dimension measurements.

Prior to X-ray diffraction analysis, specimens were ground using 1200 grade SiC. X-ray diffraction was undertaken using a Philips X'PERT system (*PW 3710*) over the  $2\theta$  range 10–100° with a step size of 0.04°. For microstructural analysis all specimens were ground on 1200 grade SiC and then successively polished on 6, 1 and 0.25  $\mu\text{m}$  diamond paste followed by OPS (colloidal Silica suspension) for 5 h. Samples were thermally etched at 1100 °C. After optical microscopy, the specimens were investigated in detail by scanning electron microscopy (Philips SEM525 equipped with an EDAX DX4 system). Additional studies were carried out under electron backscatter diffraction conditions using a Philips XL30 FEG SEM. Microwave dielectric properties were determined at 2.1 GHz by the Hakki and Coleman<sup>10</sup> method. The temperature coefficient of resonant frequency ( $\tau_f$ ) was determined by a cavity method between –20 and +60 °C.

### 3. Results and discussion

Fig. 1 shows sample densification as a function of temperature and amount of BT additions. Ceramics of 0.4CT–0.6LNT prepared without BT have an optimum

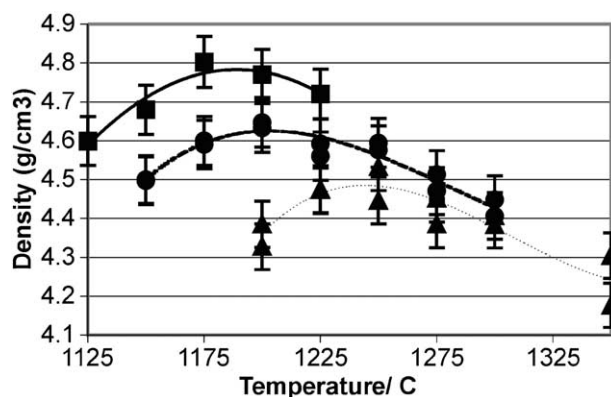


Fig. 1. Density as a function of sintering temperature for 0.4CT–0.6LNT ceramics prepared with BT additions (▲ 0 wt.%, ◆ 15 wt.%, ■ 30 wt.%).

sintering temperature of 1250 °C. Products are 95% dense, which is comparable with densities of CT–LST reported by Kim and Yoon.<sup>3</sup> However as BT is added to 0.4CT–0.6LNT the optimum sintering temperature of the solid solution decreases. The reduction is 50 °C when 30 wt.% BT is added.

Fig. 2 shows XRD spectra for un-doped 0.4CT–0.6LNT based samples. The data show that 0.4CT–0.6LNT is single phase with an orthorhombic structure. The addition of up to 15 wt.% BT to 0.4CT–0.6LNT does not result in any change in the XRD spectra from that for 0.4CT–0.6LNT. The addition of 20 wt.% BT results in the appearance of three additional peaks (31, 40 and 58.1°) indicating that the solubility limit has been exceeded with the formation of a second phase. This phase is believed to be  $\text{Bi}_4\text{Ti}_3\text{O}_{12}$ . The XRD spectra were indexed on the basis of an orthorhombic structure (Pbnm, No. 62) and show that 0.4CT–0.6LNT has in-phase, anti-phase tilting ( $a^+b^-b^-$ ) and A-site ion displacement using Glaziers classification.<sup>11</sup> Peaks 013 and 213 indicate in-phase tilting; 311, 115 and 113 indicate anti-phase tilting; peaks 021 and 210 indicate cation displacement.<sup>11</sup> The tilting mechanisms identified in un-doped 0.4CT–0.6LNT do not appear to be affected by the addition of BT.

Fig. 3 shows an SEM image of un-doped 0.4CT–0.6LNT. There is very limited porosity; the grains are predominantly rectangular in shape and 1–2  $\mu\text{m}$  in size. Fig. 4 shows an SEM image of 0.4CT–0.6LNT prepared with 15 wt.% BT and sintered at the same temperature (1225 °C) as the specimen shown in Fig. 3. The addition of BT has resulted in the appearance of very small quantities of second phase along the grain boundaries and at triple points. The total volume of second phase (Fig. 4) is below the X-ray diffraction detection limit. With higher levels of BT in the starting mixtures there are increasing amounts of second phase visible in the microstructures. At 20 wt.% BT (Fig. 5), the bismuth rich phases form needle-like structures and occasional small laths up to 3  $\mu\text{m}$  in length, and this trend is extended at 30 wt.% BT (Fig. 6). In all cases XRD analysis confirmed that the bismuth-rich second phase is  $\text{Bi}_4\text{Ti}_3\text{O}_{12}$ , in agreement with the X-ray diffraction data. The presence of significant quantities of bismuth titanate in the starting mixture leads to the formation of a liquid phase during sintering, which enables reduction of the sintering temperature, by up to 50 °C (Fig. 1). Once the solubility limit for Bi in  $0.4\text{CaTiO}_3\text{-}0.6\text{Li}_{0.5}\text{Nd}_{0.5}\text{TiO}_3$  is exceeded (above 10 wt.% BT additions) then bismuth titanate starts to form, initially as residual phases along grain boundaries, and then as distinct needles or laths in the structure.

The bismuth-rich precipitates within the grains may have formed by one of the following mechanisms. The first is during sintering where excess bismuth is rejected from the main phase when the solubility limit is

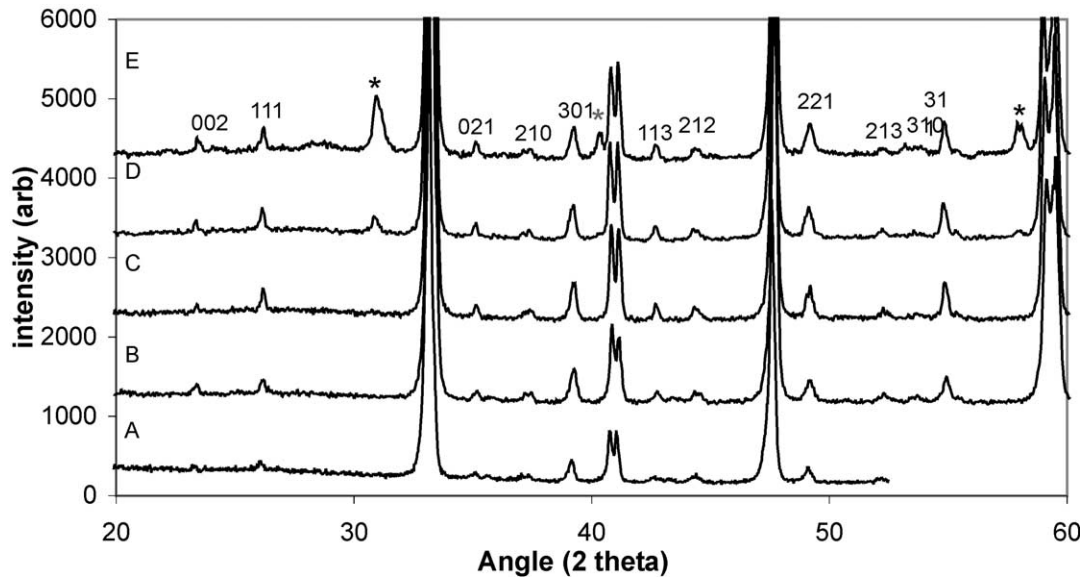


Fig. 2. X-ray diffraction spectra for 0.4CT–0.6LNT prepared with BT additions (A 0 wt.%, B 10 wt.%, C 15 wt.%, D 20 wt.%, E 30 wt.%). \*Represents peaks due to the second phase.

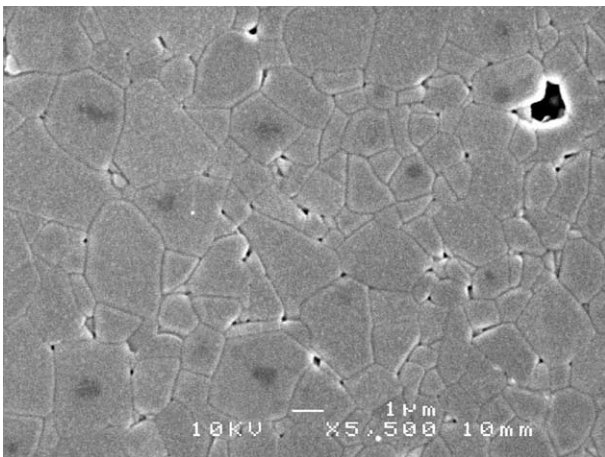


Fig. 3. SEM image of 0.4CT–0.6LNT sintered at 1225 °C for 3 h.

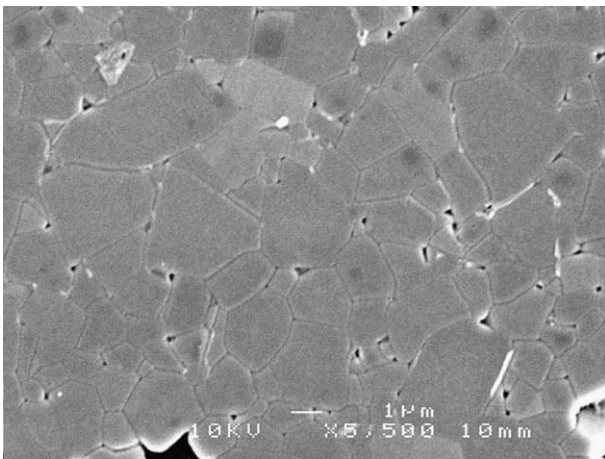


Fig. 4. SEM image of 0.4CT–0.6LNT + 15 wt.% BT sintered at 1225 °C for 3 h.

reached. The excess bismuth then nucleates on lattice defects such as twins<sup>12</sup> within the microstructure. This second phase will then tend to grow in a direction that is crystallographically controlled by the host grain. The second method is during cooling, after twinning in the microstructure has developed. At this stage there is a decrease in the solubility and the bismuth is forced out of the microstructure and into the twins, which can act as both impurity sinks and high diffusion pathways.<sup>13</sup> Whilst only a small amount of bismuth may diffuse in to the twins, the small area of the twins will result in a high bismuth concentration.

Fig. 7 shows that undoped 0.4CT–0.6LNT has a relative permittivity of 126 and a  $Q \times f$  value of 2600

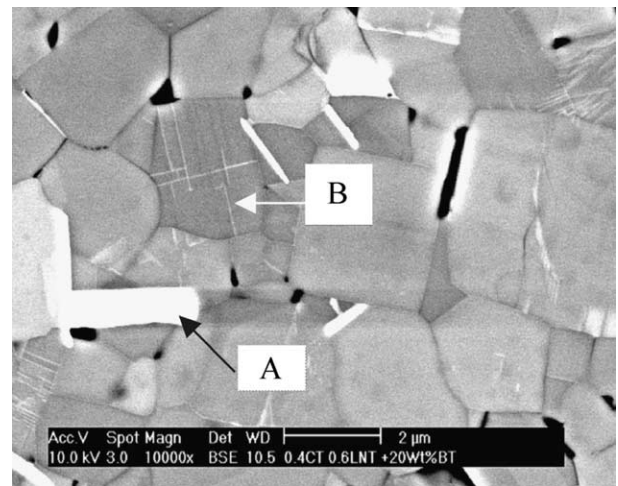


Fig. 5. SEM image of 0.4CT–0.6LNT + 20 wt.% BT sintered at 1175 °C for 3 h: A shows a bismuth-rich second phase and B indicates a bismuth-rich needles within a grain.



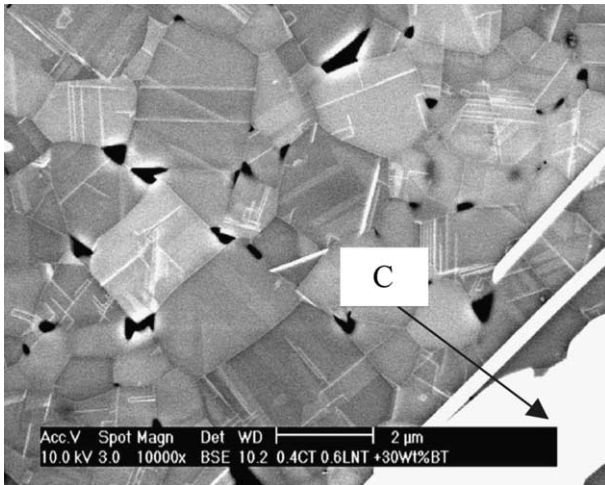


Fig. 6. SEM image of 0.4CT–0.6LNT+30 wt.% BT sintered at 1175 °C for 3 h; C shows the large bismuth-rich second phase.

GHz (measured at 2.1 GHz). This is close to the value predicted by Takashi et al.<sup>6</sup> when Sm is replaced by Nd. It is noted that the substitution of Sm by Nd in CT–LST increases the relative permittivity<sup>3</sup> from 120 to 126 but is accompanied by a decrease in the  $Q \times f$ . from around 4000 GHz (at 5 GHz) in 0.4CaTiO<sub>3</sub>–0.6Li0.5Sm0.5TiO<sub>3</sub> to 2600 GHz in 0.4CaTiO<sub>3</sub>–0.6Li0.5Nd0.5TiO<sub>3</sub>.

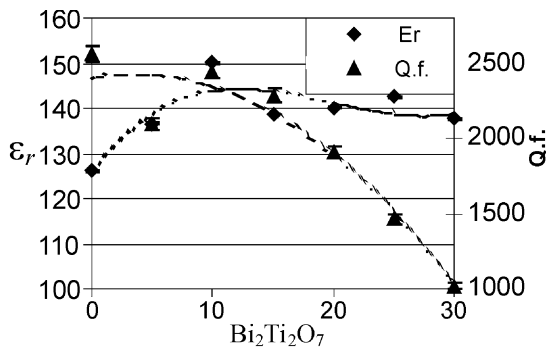


Fig. 7.  $Q \cdot f$  ( $\pm 2.0\%$ ) and  $\epsilon_r$  ( $\pm 0.1\%$ ) as a function of BT addition to 0.4CT–0.6LNT.

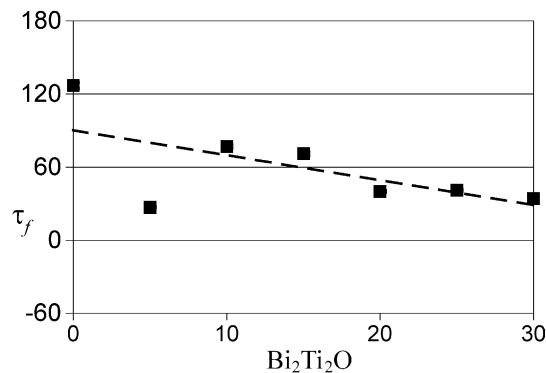


Fig. 8.  $\tau_f$  (ppm/°C  $\pm 2.0\%$ ) as a function of BT addition to 0.4CT–0.6LNT.

The addition of up to 10 wt.% BT to 0.4CT–0.6LNT (Fig. 7) results in a significant increase in the relative permittivity up to 150, but at higher levels of BT there is a slight reduction in  $\epsilon_r$ . In contrast, small additions (up to 10 wt.%) BT to 0.4CT–0.6LNT result in a small decrease in the  $Q \cdot f$ . (2600–2450 GHz) but higher levels result in a severe decrease in the  $Q \cdot f$ . value (down to 1000 GHz at 30 wt.% BT). The temperature coefficient of resonant frequency ( $\tau_f$ ) in undoped 0.4CT–0.6LNT is 127 ppm/°C (Fig. 8). As BT is added to 0.4CT–0.6LNT,  $\tau_f$  decreases, almost linearly, to 34 ppm/°C at 30 wt.% BT (Fig. 8).

Therefore small additions of BT to the 0.4CT–0.6LNT system, up to 10 wt.%, result in a significant increase in the relative permittivity, a small decrease in the  $Q \cdot f$ . and a beneficial decrease in  $\tau_f$  towards zero. As such, small additions of BT to CT based microwave ceramic systems offer potential as a mechanism for tuning the  $\tau_f$  and simultaneously enhancing the relative permittivity of the material.

Good quality ceramics of 0.4CaTiO<sub>3</sub>–0.6Li0.5Nd0.5TiO<sub>3</sub> were prepared by the mixed oxide route. Small additions of BT to 0.4CT–0.6LNT resulted in a significant increase in the relative permittivity, a small decrease in the  $Q \cdot f$ . value and decrease in  $\tau_f$  towards zero. At higher levels of BT additions, second phases, rich in bismuth develop as needles and then laths within the primary grains. This is accompanied by a small reduction in  $\epsilon_r$ , a significant reduction in  $Q \cdot f$  and a linear reduction in  $\tau_f$  towards zero. Small additions of Bismuth Titanate may be used to tune the microwave properties of 0.4CT–0.6LNT, to yield ceramics with optimum microwave properties.

## Acknowledgements

The provision of an EPSRC Doctoral Training Award to T Lowe and the support of Filtronic Comtek are gratefully acknowledged.

## References

1. Ubic, R., Reaney, I. M. and Lee, W. E., Microwave dielectric solid-solution phase in system BaO–Ln<sub>2</sub>O<sub>3</sub>–TiO<sub>2</sub> (Ln = lanthanide cation). *International Materials Reviews*, 1998, **43**, 205–219.
2. Woo Sup, Kim and Ki, Hyun Yoon, Microwave dielectric properties and far-infrared reflectivity characteristics of the CaTiO<sub>3</sub>–Li<sub>0.5–3x</sub>Sm<sub>0.5+x</sub>TiO<sub>3</sub> ceramics. *J. Am. Ceram. Soc.*, 2000, **83**(9), 2327–2329.
3. Woo Sup, Kim, Ki, Hyun Yoon and Eung, Soo Kim, Far-infrared reflectivity spectra of CaTiO<sub>3</sub>–Li<sub>0.5</sub>Sm<sub>0.5</sub>TiO<sub>3</sub> microwave dielectrics. *Materials Research Bulletin*, 1999, **34**, 2309–2317.
4. Ki, Hyun Yoon, Yoon, Chang, Woo Sup, Kim, Jae, Beom Kim and Eung, Soo Kim, Dielectric properties of Ca<sub>1–x</sub>Sm<sub>2x/3</sub>TiO<sub>3</sub>–Li<sub>0.5</sub>Sm<sub>0.5</sub>TiO<sub>3</sub> ceramics. *Jpn. J. Appl. Phys.*, 1996, **35**, 5145–5149.
5. Jeong-Seog, Kim, Chae-Il, Cheon, Hyun-Joo, Kang, Chang-Hee,

- Lee, Kyung-Yong, Kim, Sahn, Nam and Jae-Dong, Byun, Crystal structure and microwave dielectric properties of  $\text{CaTiO}_3$ – $(\text{Li}_{0.5}\text{Sm}_{0.5})\text{TiO}_3$ – $(\text{Ln}_{1/3}\text{Nd}_{1/3})\text{TiO}_3$  (Ln = La, Dy) ceramics. *Jpn. J. Appl. Phys.*, 1999, **38**, 5633–5637.
6. Takashi, H., Baba, Y., Ezaki, K. and Shibata, K., Microwave dielectric properties and crystal structure of  $\text{CaO}$ – $\text{Li}_2\text{O}$ – $(1-x)\text{Sm}_2\text{O}_3$ – $x\text{Ln}_2\text{O}_3$ – $\text{TiO}_2$  (Ln: Lanthanide) ceramic system. *Jpn. J. Appl. Phys.*, 1996, **35**, 5069–5073.
  7. Valant, M., Suvorov, D. and Kolar, D., Role of  $\text{Bi}_2\text{O}_3$  in optimising the dielectric properties of  $\text{Ba}_{4.5}\text{Nd}_9\text{Ti}_{18}\text{O}_{54}$  based microwave ceramics. *J. Mater. Res.*, 1996, **11**, 928–931.
  8. Wersing, W. *Electronic Ceramics*. Elsevier Sci. Pub., 1991.
  9. Durand, J. and Boilot, J., Microwave characteristics of  $\text{BaO}$ – $\text{Bi}_2\text{O}_3$ – $\text{TiO}_2$ – $\text{Nd}_2\text{O}_3$  dielectric resonators. *J. Mater. Sci. Lett.*, 1987, **6**(2), 134–136.
  10. Hakki, B. and Coleman, P., A dielectric resonator method of measuring inductive capacities in the millimeter range. *IRE Trans. On Microwave Theory and Techniques*, 1960, **MTT-8**, 402–410.
  11. Glazer, A., Simple ways of determining perovskite structures. *Acta Cryst.*, 1975, **A31**, 756–762.
  12. Young-Sung, Yoo, Hwan, Kim and Doh-Yeon, Kim, Effect of  $\text{SiO}_2$  and  $\text{TiO}_2$  addition on the exaggerated grain growth of  $\text{BaTiO}_3$ . *J. Eur. Ceram. Soc.*, 1997, **17**(6), 805–811.
  13. Salje, E. K. H., Mesoscopic structures in ferroelastic and co-elastic materials. *Ferroelectrics*, 2002, **267**, 113–120.